

Total broadband control of far-field diffraction patterns with metagratings

Vladislav Popov*

SONDRA, CentraleSupélec, Université Paris-Saclay, F-91190, Gif-sur-Yvette, France

Fabrice Boust†

SONDRA, CentraleSupélec, Université Paris-Saclay, F-91190, Gif-sur-Yvette, France and
ONERA - The French Aerospace Lab, 91120, Palaiseau, France

Shah Nawaz Burokur‡

LEME, UPL, Univ Paris Nanterre, F92410, Ville d'Avray, France

In this study, metagratings are used to achieve total control over electromagnetic waves diffracted in the far-field. To this end, we consider a 1D periodic array of super cells composed of N polarization electric line currents placed over a grounded dielectric substrate and excited by an incident plane wave. To validate the developed theoretical approach, broadband anomalous and multichannel reflections are demonstrated from 3D full-wave simulations in the microwave regime at 10 GHz.

For long time, the microwave community has approached a particular problem of anomalous reflections by means of reflectarray antennas [1, 2]. In such reflectarray antennas, a linear phase variation is created along the surface, allowing one to reflect incident waves to a desirable angle. With the development of nanofabrication techniques and metasurfaces, the concept of reflectarrays was transposed to infra-red and optical frequency domains [3, 4]. A metasurface is represented by a 2D dense distribution of subwavelength scatterers and a reflectarray is a particular case of a metasurface which can generally be used for various applications other than anomalous reflections. However, reflectarrays suffer from low efficiencies for angles of anomalous reflection approximately greater than 45 degrees [5]. Stimulated by the advances in fabrication techniques, extensive research in the area established a strong theoretical ground in the form of equivalence principle [6] for the design of wavefront manipulation devices based on the use of metasurfaces. Very recently a metasurface performing highly efficient anomalous reflection at steep angle has been demonstrated in [7] on the basis of the concept of spatially dispersive metasurfaces [5, 8].

In spite of theoretical advances in the field of metasurfaces, drawbacks concerning design complexity and material losses still exist, rendering implementation of high performance devices very challenging in some frequency ranges [9].

In this study we propose to use the recent concept of metagratings [10] for the manipulation of reflected waves. Basically, a metagrating is a set of 1D arrays of scatterers such as polarization line currents, separated by a distance of the order of the operating wavelength λ . Metagratings allow one to significantly decrease the number of constitutive scatterers in contrast to metasurfaces where scat-

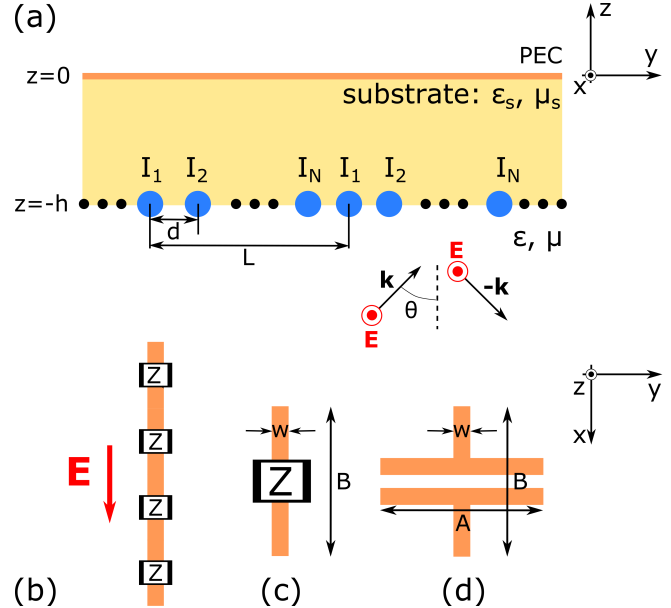


FIG. 1. (a) System under consideration: a periodic array of line currents $\mathbf{J}_{nq} = I_q \exp[-jk \sin[\theta]nL] \delta(y - y_{nq}, z + h)\mathbf{x}_0$ (blue circles) placed on PEC-backed dielectric substrate having permittivity ϵ_s , permeability μ_s and thickness h . The array is excited by a plane wave incident at angle θ and having TE polarization. (b) A line current implemented as a 1D array of loaded dipoles. (c) A PEC strip dipole of length B and width w loaded with lumped impedance Z . (d) A PEC strip dipole loaded with printed circuit capacitance having arms of length A .

terers are tightly packed in the plane. This reduction can be very attractive to reduce the fabrication complexity as well as joule losses.

It has been already shown that having just a single line current per period is capable to perform perfect beam splitting and retroreflection [10–12]. Chalabi *et al.* also demonstrated the possibility to perform near-perfect anomalous reflection using two line currents per super

* uladzislau.popov@centralesupelec.fr

† fabrice.boust@onera.fr

‡ sburokur@parisnanterre.fr

cell [13]. Recently, an implementation of a graphene-based tunable metagrating operating in the THz frequency range was suggested in [14].

In the present work, we study a general case of metagratings having N polarization line currents per super cell. This generalization allows one to control all electromagnetic waves scattered from a metagrating in the far-field and is able to perform transformations of the incident wave such as near-perfect anomalous reflection, beam splitting, multichannel reflection and so on. It also includes small-angle anomalous reflection which is not accessible with metagratings that have been considered so far in the literature.

As physical system, we consider a 1D periodic array of polarization electric line currents placed over a grounded dielectric substrate of thickness h and excited by an incident harmonic TE-polarized plane wave at angle θ where $\exp[j\omega t]$ time dependence is assumed. The array has period L and consists of super cells each having N equally separated line currents by the distance $d = L/N$. The schematics of the considered system is presented in Fig. 1 (a). A line current is imagined as a tightly packed row of point dipoles orientated in the same direction, see Fig. 1 (b). Practically, one can realize the dipoles as the loaded rods considered in Fig. 1 (c) and (d).

In the presence of the grounded substrate the excitation field takes the following form

$$E_x^{exc}(y, z \leq -h) = \left(e^{-j\beta_0 z} + R_0^{TE} e^{j\beta_0(z+2h)} \right) e^{-jk \sin[\theta]y}. \quad (1)$$

Electric line currents in the array are represented as current densities $\mathbf{J}_{nq}(\mathbf{r}) = I_q \exp[-jk \sin[\theta]nL] \delta(y - y_{nq}, z + h) \mathbf{x}_0$ where $\delta(y, z)$ is the Dirac delta function, $y_{nq} = nL + (q-1)d$, n and q take integer values from $-\infty$ to $+\infty$ and from 1 to N , respectively. The term $\exp[-jk \sin[\theta]nL]$ represents the phase variation of the currents introduced by the incident wave. Radiation of the array of electric line currents is represented by a series of Hankel functions [15, 16] of the second kind. It can be shown by means of the Poisson's formula that the electric field radiated by the array outside the substrate can be written as

$$E_x(y, z < -h) = -\frac{k\eta}{2L} \sum_{m=-\infty}^{+\infty} \frac{\rho_m^{(I)}}{\beta_m} (1 + R_m^{TE}) e^{-j\xi_m y} e^{j\beta_m(z+h)},$$

$$E_y = E_z = 0. \quad (2)$$

Corresponding magnetic fields can be found by means of Maxwell's equations. The series represent superpositions of plane waves having tangential component of wave vector equal to $\xi_m = k \sin(\theta) + 2\pi m/L$, the longitudinal component is given by $\beta_m = \sqrt{k^2 - \xi_m^2}$ outside and by $\beta_m^s = \sqrt{k_s^2 - \xi_m^2}$ inside the substrate [$k = \omega\sqrt{\epsilon\mu}$ and $k_s = \omega\sqrt{\epsilon_s\mu_s}$ are respectively the wave numbers outside

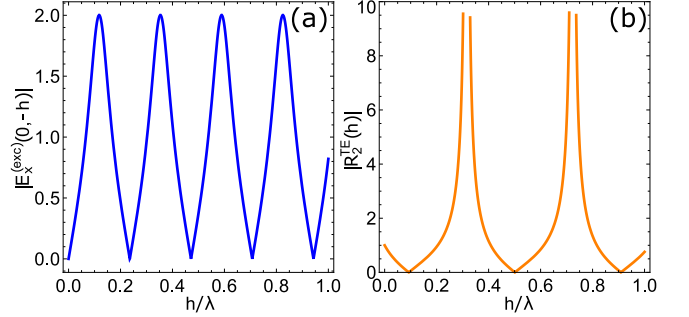


FIG. 2. (a) Dependence of the excitation field [$\theta = 0$] acting on a metagrating on the thickness of the substrate h when $\epsilon_s = 4.5$ and $\mu_s = 1$. (b) Absolute values of the R_2^{TE} vs. the thickness of the substrate when $\theta = 0$, $r = l = 1$, $N = 3$ and $L = \lambda/\sin[60^\circ]$. The rest of R_m^{TE} does not have poles under these parameters. λ is the operating vacuum wavelength.

and inside the substrate]. Thus, R_m^{TE} is Fresnel's reflection coefficient

$$R_m^{TE} = \frac{j\gamma_m^{TE} \tan[\beta_m^s h] - 1}{j\gamma_m^{TE} \tan[\beta_m^s h] + 1}, \quad \gamma_m^{TE} = \frac{k_s \eta_s \beta_m}{k \eta \beta_m^s}, \quad (3)$$

where $\eta = \sqrt{\mu/\epsilon}$ and $\eta_s = \sqrt{\mu_s/\epsilon_s}$. Each current contributes to the amplitudes of the plane waves via the introduced quantity $\rho_m^{(I)}$

$$\rho_m^{(I)} = \sum_{q=1}^N I_q \exp[j\xi_m(q-1)d]. \quad (4)$$

One can recognize in Eq. (4) a discrete Fourier transformation.

In general case when a plane wave illuminates a metagrating one can find $r + l + 1$ scattered plane waves in the far-field, where r and l are largest integers satisfying the conditions $\beta_r \geq 0$ and $\beta_{-l} \geq 0$. However, we can arbitrary control all of the $r + l + 1$ plane waves if the number N of line currents in a super cell is equal to $r + l + 1$. Indeed, amplitude A_m^{TE} of the m^{th} plane wave depends on $\rho_m^{(I)}$ which is determined by the currents I_q [see Eq. (2)]

$$A_m^{TE} = \rho_m^{(I)} \frac{(1 + R_m^{TE}) e^{j\beta_m h}}{\beta_m} + \delta_{m0} R_0^{TE} e^{2j\beta_0 h}, \quad (5)$$

where δ_{m0} is the Kronecker delta accounting for the incident wave reflected from the substrate. By setting all the amplitudes A_m^{TE} ($m \in [-l, r]$), one can find necessary I_q from the corresponding $\rho_m^{(I)}$ which are related via Eq. (4). Thus, by designing currents I_q one can perform all possible transformations of the far-field diffraction pattern, e.g. beam splitting, anomalous reflection, multichannel reflection, etc.

Necessary currents I_q can be achieved by engineering the line currents impedance densities $Z_q = I_q E_x^{(loc)}(y_{0q}, -h)$, where $E_x^{(loc)}(y_{0q}, -h)$ is the total electric field at the location of the q^{th} line current [$y_{0q} =$

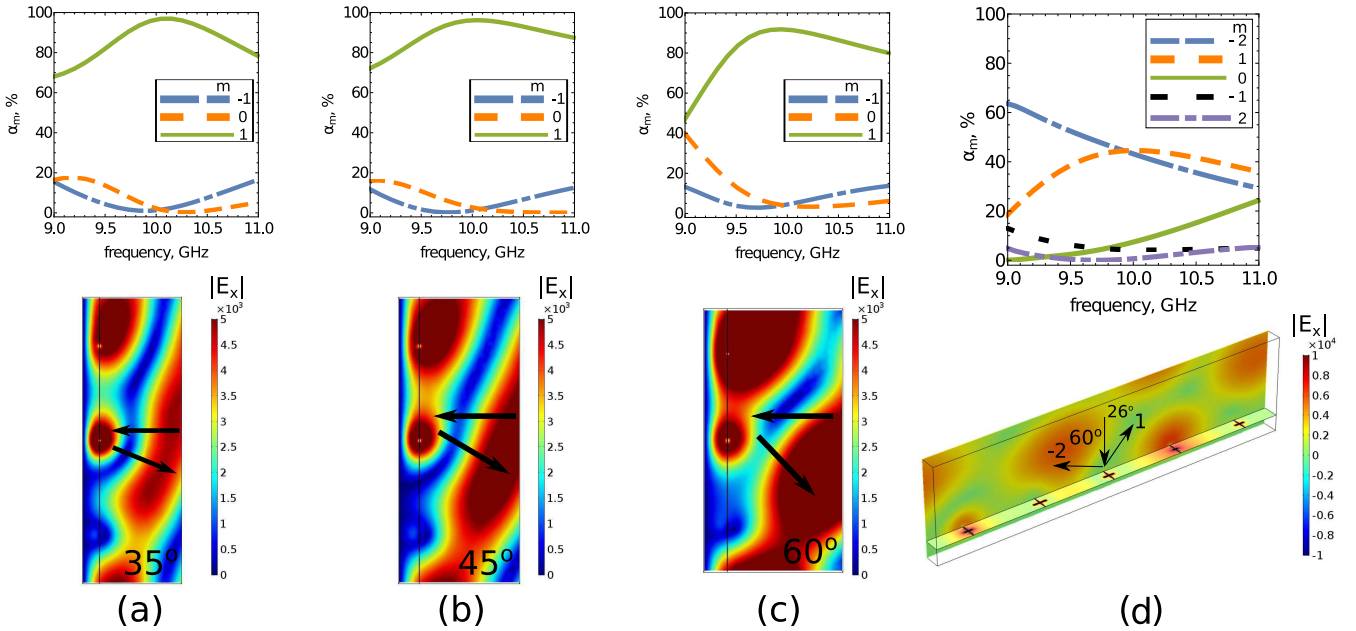


FIG. 3. (a)–(c) 3D full-wave simulations of anomalous reflection realized with metagratings having $N = 3$ electric line currents implemented as loaded strips. Super cell's period for each case is calculated as $L = \lambda / \sin[\theta_r]$. For (a) $\theta_r = 35^\circ$ and (b) $\theta_r = 45^\circ$ impedance densities [in η/λ] are $Z_1 = -j14.5$, $Z_2 = -j7.69$, $Z_3 = -j5.44$ and (c) $\theta_r = 60^\circ$ $Z_1 = -j13.7$, $Z_2 = -j7.41$, $Z_3 = -j4.53$. (d) Splitting of the normally incident wave equally between the minus second $[-60^\circ]$ and first diffraction orders $[26^\circ]$ with the super cell's period being $L = 2\lambda / \sin[60^\circ]$, impedance densities [in η/λ] are $Z_1 = -j6.77$, $Z_2 = -j4.03$, $Z_3 = -j5.08$, $Z_4 = -j9.71$, $Z_5 = -j5.45$. The top row of figures demonstrate frequency response of metagratings' transformation efficiency designed to operate at 10 GHz. The bottom row depicts corresponding electric field snapshots at 10 GHz.

$(q-1)d$, $z = -h$]. The impedance densities Z_q can be calculated by means of the following formula [in the same way as it is done in [12] for a particular case of $N = 1$]

$$Z_q = \frac{1}{I_q} \left[E_x^{(exc)}(y_{0q}, -h) - \frac{k\eta}{4} \sum_{t=1, t \neq q}^N \sum_{n=-\infty}^{\infty} I_t e^{-jk \sin[\theta] n L} \right. \\ \times H_0^{(2)}[k|(q-t)d - nL|] - \frac{k\eta}{2L} \sum_{t=1}^N \sum_{m=-\infty}^{+\infty} I_q e^{j\xi_m(t-q)d} \frac{R_m^{TE}}{\beta_m} \left. \right] \\ - \frac{k\eta}{2} \sum_{n=1}^{\infty} \cos[k \sin[\theta] n L] H_0^{(2)}[k|nL|] - \frac{k\eta}{4} H_0^{(2)}[kr_0], \quad (6)$$

where $H_0^{(2)}[y, z]$ is the Hankel function of the second kind and r_0 is the effective radius of the line current which depends on its concrete practical realization. For instance, when a line current is imitated as a strip of width w the radius $r_0 = w/4$ [16].

In a general case, currents found from (5) correspond to active and lossy impedance densities Z_q calculated from (6). From a practical point of view, we are interested only in passive and lossless metagratings where $\Re[Z_q] = 0$, which cannot radiate energy by themselves and do not require engineered joule losses. Thus, a metagrating basically redistributes the energy of the incident wave between $r + l + 1$ diffracted in the far-field plane waves. Then it is clear that the power conservation condition when assuming a unity amplitude of the incident

wave reads as

$$\sum_{m=-l}^r \alpha_m = 1, \quad \alpha_m = |A_m^{TE}|^2 \frac{\beta_m}{\beta_0}, \quad (7)$$

where α_m is the part of the incident energy going in the m^{th} diffraction order.

In contrast to the case of metagratings having a single line current in a super cell [10–12], here we deal with a very general configuration of metagratings making it impossible to analytically derive [because of Hankel functions in the square brackets of Eq. (6)] conditions on currents I_q ensuring $\Re[Z_q] = 0$ when condition (7) is satisfied. Instead, we develop a very simple real valued genetic algorithm [17] which allows one to find reactive impedance densities Z_q having $\Re[Z_q] = 0$ with given impedance reactivity accuracy p for a desired far-field diffraction pattern obtained with given transformation accuracy α . The impedance reactivity accuracy is defined in accordance with the following inequality

$$\sqrt{\sum_{q=1}^N \left| \frac{\Re[Z_q]}{Z_q} \right|^2} < p. \quad (8)$$

A far-field diffraction pattern is set by assigning to all α_m^0 certain values. Phases $\phi_m = \arg[A_m^{TE}]$ are assumed to be not important and assigned randomly. Transformation accuracy α means that one is satisfied with a transformation when the part of the incident energy going in the m^{th}

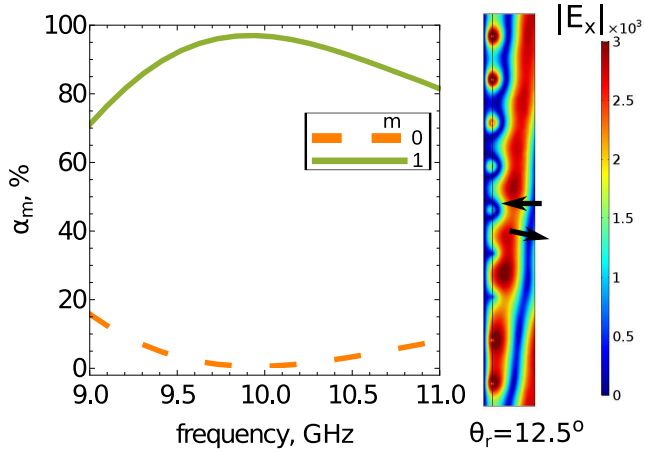


FIG. 4. 3D full-wave simulation of small angle anomalous reflection [12.5°] realized with metagratings having $N = 9$ electric line currents implemented as loaded strips. Super cell's period is calculated as $L = 4\lambda/\sin[60^\circ]$ and impedance densities [in η/λ] were found as $Z_1 = -j7.62$, $Z_2 = -j6.96$, $Z_3 = -j6.19$, $Z_4 = -j5.55$, $Z_5 = -j5.18$, $Z_6 = -j3.57$, $Z_7 = -j3.02$, $Z_8 = -j18.7$, $Z_9 = -j10.1$. The left part of the figure demonstrates frequency response of metagratings design for 10 GHz. The right part of the figure depicts electric field snapshots at 10 GHz.

diffraction order is within the range $\alpha_m = \alpha_m^0 \pm \alpha$. Still, at each step the genetic algorithm deals with $\alpha_m > 0$ constrained by the energy conservation condition (7).

When designing a metagrating, one should also take care of choosing parameters of the substrate. First of all, when substrate's thickness is varied the value of the excitation field Eq. (1) on a metagrating passes through zeros as illustrated in Fig. 2 (a). Clearly, a metagrating cannot be excited when the excitation field is zero on its plane. And secondly, the reflection coefficient R_m^{TE} as a function of h has poles when m is such that $k < \xi_m$ but $k_s > \xi_m$ [Fig. 2 (b)]. The poles correspond to excitation of waveguide modes inside the substrate. Thus, assuming ε_s and μ_s of the substrate are set, one should choose the thickness: (i) corresponding to vicinity of the maximum of the excitation field on a metagrating and (ii) $|R_m^{TE}(h)| \neq \infty$.

In order to validate the developed theoretical basis, we perform full-wave simulations with *COMSOL Multiphysics*. One can realize the line currents as dense 1D arrays of loaded dipoles [separated by distance $B \ll \lambda$ and having lumped load equal to Z] as in Figs. 1 (b) and (c). Then, the impedance density is simply Z/B . The load can be realized as a printed circuit capacitance as illustrated in Fig. 1 (d) for which $Z = -j\eta\kappa/(A\varepsilon_{eff})$ [when other parameters B and w are fixed], κ is the proportionality factor which is the same for all line currents in a super cell and found from full-wave 3D simulations,

ε_{eff} is approximated as $(1 + \varepsilon_s)/2$ and μ_s is assumed equal to 1.

We demonstrate three examples of metagratings operating at 10 GHz [$\lambda \approx 30$ mm]: (i) having $N = 3$ and performing anomalous reflection at angle θ_r [Figs. 3 (a) – (c)]; (ii) having $N = 5$ and equally redistributing the incident energy between the minus second $m = -2$ and the first $m = 1$ diffraction orders [Fig. 3 (d)] and (iii) performing small-angle anomalous reflection with metagrating having $N = 9$ [Fig. 4]. In all cases, normally incident plane wave is assumed, i.e. $\theta = 0$. Parameters of the dielectric substrate correspond to commercially available Arlon AD450 substrate: $\varepsilon_s = 4.5$, $\mu_s = 1$ and $h = 3$ mm. For the genetic algorithm, the impedance reactivity accuracy was set to 1% for the first two cases and to 10% for the third one. The transformation accuracy was set to 5% in all cases. A polarization line current is implemented as a 1D array of loaded flat strips [as seen from Fig. 3 (d)]. We find parameter κ equals approximately 2.794 mm for the loaded flat strips in all considered cases [assuming $B = \lambda/10 = 3$ mm and $w = 3\text{mil} \approx 76.2\mu\text{m}$] which realize necessary impedance densities Z_q with $A_q = -\tilde{\kappa}/(\Im[Z_q]\frac{\lambda}{\eta}\varepsilon_{eff})$, $\tilde{\kappa} = \lambda\kappa/B$. The results of 3D simulations are summarized in Figs. 3 and 4.

In conclusion, it has been shown that a metagrating having the number of polarization line currents per super cell equal to the number of plane waves scattered in the far-field can be used for total control of the far-field diffraction patterns. Namely, equations (4) and (5) allowing one to find currents realizing desirable transformations have been derived. Since analytical formulas for the impedance densities (6) are not applicable for direct design, genetic algorithms have been implemented for that purpose.

The diffraction orders control has been demonstrated by means of 3D full-wave simulations on the examples of anomalous reflection [at small and steep angles] and equal redistribution of the energy of the incident wave between two diffraction orders. From Figs. 3 and 4, one can clearly observe that metagratings can operate in a wide frequency band in comparison to conventional metasurfaces which are inherently resonant. However, one should keep in mind that when changing frequency one also changes the scattering angles.

The validation results can be very interesting for the metamaterials community to perform highly efficient control of light scattering. It allows one to significantly decrease the number of used elements and simplify the design, which is very convenient for optical and infra-red frequency ranges. Our findings also may serve as a way for development of efficient tunable antennas in the microwave domain.

[1] S. V. Hum, M. Okoniewski, and R. J. Davies, IEEE Microwave and Wireless Components Letters **15**, 422 (2005).

[2] S. V. Hum, M. Okoniewski, and R. J. Davies, IEEE Transactions on Antennas and Propagation **55**, 2200 (2007).

[3] N. Yu, P. Genevet, M. A. Kats, F. Aieta, J.-P. Tetienne, F. Capasso, and Z. Gaburro, Science **334**, 333 (2011).

[4] S. B. Glybovski, S. A. Tretyakov, P. A. Belov, Y. S. Kivshar, and C. R. Simovski, Physics Reports **634**, 1 (2016).

[5] V. S. Asadchy, M. Albooyeh, S. N. Tcvetkova, A. Díaz-Rubio, Y. Ra'di, and S. A. Tretyakov, Phys. Rev. B **94**, 075142 (2016).

[6] C. Pfeiffer and A. Grbic, Physical Review Letters **110**, 1 (2013).

[7] A. Díaz-Rubio, V. S. Asadchy, A. Elsakka, and S. A. Tretyakov, Science Advances **3** (2017), 10.1126/sciadv.1602714.

[8] A. Epstein and G. V. Eleftheriades, Phys. Rev. Lett. **117**, 256103 (2016).

[9] B. Ratni, A. de Lustrac, G.-P. Piau, and S. N. Burokur, Opt. Express **26**, 2613 (2018).

[10] Y. Ra'di, D. L. Sounas, and A. Alù, Phys. Rev. Lett. **119**, 067404 (2017).

[11] A. Epstein and O. Rabinovich, Phys. Rev. Applied **8**, 054037 (2017).

[12] O. Rabinovich and A. Epstein, arXiv preprint arXiv:1801.04521 (2018).

[13] H. Chalabi, Y. Ra'di, D. L. Sounas, and A. Alù, Phys. Rev. B **96**, 075432 (2017).

[14] Y. Ra'di and A. Alù, ACS Photonics **0**, null (0).

[15] L. B. Felsen and N. Marcuvitz, *Radiation and scattering of waves*, Vol. 31 (John Wiley & Sons, 1994).

[16] S. Tretyakov, *Analytical modeling in applied electromagnetics* (Artech House, 2003).

[17] A. H. Wright (Elsevier, 1991) pp. 205 – 218.